CALIBRATION AND SIMULATION OF THE LCLS UNDULATOR BEAM LOSS MONITORS USING APS ACCELERATORS*

J.C. Dooling†, W. Berg, A. Brill, L. Erwin, and B.-X. Yang, ANL, Argonne, IL 60439, USA
A.S. Fisher, H.-D. Nuhn, and M. Santana Leitner, SLAC, Menlo Park, CA 94025, USA

Abstract

Electrons scattered by alumina ceramic transverse beam profile monitors inserted in the Advanced Photon Source (APS) booster-to-storage ring (BTS) transfer line are used to generate Čerenkov light for calibration of beam loss monitors (BLMs) installed in the Linac Coherent Light Source (LCLS) undulator beamline. In addition, gas bremsstrahlung (GB) photons generated by 7-GeV electrons in the APS sector 35 storage ring straight section are used to create pair-production electrons for measurement and calibration purposes. Both cases are modeled with the particle-matter interaction program MARS. The realized tuning fork geometry of the BLM exhibits regions of greater sensitivity in the radiator. Transverse GB beam scans have provided uniformity and sensitivity data throughout the volume of the radiator. Comparisons between predicted and measured signal strengths and thermoluminescent dosimeter readings are given and shown to be in reasonable agreement.

STATUS

Installation of the 33 undulator Čerenkov beam loss monitors (BLMs) was completed in FY2010. All are now integrated into the LCLS machine protection system (MPS). In addition to providing machine protection, we have considered using the BLMs to provide dosimetry for the undulator permanent magnets. Dosimetry requires calibration of the BLM system, which is accomplished through measurements and simulations. Detector calibration data is sought in terms of output charge for a given input charge incident on the BLM; we then use simulations to tie electron fluence in the radiators to neutron and star fluence in the magnets. Čerenkov beam loss monitors are good at detecting low levels of electron fluence; however, they are poor indicators of energy. Both fluence and energy are needed to determine dose; therefore simulations must be relied upon to provide average energy and energy deposition. This calibration effort is on-going.

CALIBRATIONS AND SIMULATIONS

BLM testing was initially considered in three separate areas of the Advanced Photon Source (APS) where beam loss can be created or is known to occur. These locations are 1) booster to storage ring (BTS) transport line, 2) storage ring (SR) undulator straight section, and 3) photon beamline where gas bremsstrahlung photons may be used to create pair production electrons and positrons. We are looking for locations where lost particles would be of relevant energies (E_{max} >4.3 GeV) and the loss pattern has desirable spatial characteristics. Specifically, we are looking for the loss pattern to be either broad, and therefore illuminate the BLM uniformly, or narrow enough to allow mapping of the optical coupling efficiency across transverse positions of the monitor. Simulations and subsequent data show that beam loss in the SR straight section is not uniform and tends to concentrate on the inside of the vacuum chamber; therefore, we did not pursue these measurements beyond initial tests.

In earlier work [1] comparing beam finder wire (BFW) measurements with simulations of an LCLS model, we found an optical coupling coefficent of approximately 1.4×10^{-3} in the large cross section of the BLM. In this paper, we compare this result with data recorded at the APS.

BTS

A broad loss pattern was created in the upstream region of the BTS by introducing 0.5-mm-thick alumina flags into the path of 7-GeV electrons extracted from the booster synchrotron. The flags are part of a set employed by APS operators to perform initial beam alignment in the BTS; the elements used in this study are positioned 12 m (FS1) and 20 m (FS2) upstream of the BLM location. The BLM is placed within a shield constructed of $5.1\times10.2\times20.3$ cm^3 Pb bricks 21 m downstream of the booster extraction kicker magnet. The BLM is mounted to a pneumatically driven, linear slide that raises the monitor 15.2 cm out of the shield when exposure is desired. During dedicated machine studies, thermoluminescent dosimeters (TLDs) were placed on and around the BLM and the Pb shield bricks. A footprint of the Pb shield with TLD locations is shown in Figure 1.

Electron bunches were continuously extracted from the booster synchrotron at a 2-Hz rate while flags FS1 and FS2 were separately inserted into the beam. Over a period of approximately 70 minutes, the BLM was raised out of the Pb shield and exposed to the shower created by each of the two flags. TLD data recorded from the study are presented in Table 1 and compared with the results of MARS simulations. The position numbers given in the table refer to the locations shown in Fig. 1.

During the BTS study, FS1 flag was inserted into the beam for 42.25 minutes and FS2 flag for 27.27 minutes; over these periods the total charges extracted were 8946 nC and 5540 nC. Simulations predict TLD dose rates for both cases. During the study, Čerenkov light pulses induced by

* Work supported by the U.S. Department of Energy, Office of Science, Office of Basic Energy Sciences, under contract number DE-AC02-06CH11357.

† dooling@aps.anl.gov

This material is based upon work supported by the U.S. Department of Energy, Office of Science, Office of Basic Energy Sciences, under Contract No. DE-AC02-76SF00515.

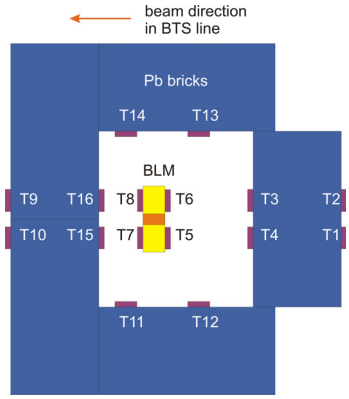

Figure 1: Plan view of TLD placement on the BLM and Pb shield.

Table 1: BTS TLD and MARS Total Dose Equiv. Readings

TLD #	D_{eq} (mSv)	MARS (mSv)	TLD #	D_{eq} (mSv)	MARS (mSv)
1	66.3	98.5	9	17.9	4.6
2	34.3	92.0	10	19 5	1.6
3	4.6	5.7	11	6.8	14.0
4	7.0	3.2	12	7.8	16.4
5	79.9	115.4	13	6.3	28.1
6	145.1	112.7	14	6.4	6.9
7	80.3	146.7	15	8.3	115.4
8	118.1	114.3	16	6.1	7.0

beam loss are recorded as a function of high-voltage bias on the photomultiplier tube (PMT).

Figure 2 shows loss pulses with flag 2 inserted into the beam for PMT bias voltages of -500 V and -700 V. Afterpulse effects are evident at higher PMT voltages (gain). Afterpulses may result following short, high-intensity light signals [2, 3]. The figure shows 120 waveforms superimposed for each bias case representing 1 minute of data at 2 Hz. The afterpulse relative amplitude is clearly voltage dependent. Afterpulsing is statistical, so integrating the afterpulse should not help the measurement. Typically, the LCLS BLM HV is set to -500 V, sufficient to provide adequate gain, yet low enough not to provoke afterpulsing.

An original set of five undulator BLMs were installed in 2009. When the full complement of 33 BLMs were delivered and installed in FY2010 replacement fused-silica radiators were used. The new radiators show better optical coupling efficiency. Initial tests in the BTS were conducted with the original set of radiators. Figure 3 provides a comparison of measured PMT output charge versus high-voltage bias for the two flags. We note that the new glass never appears to follow the 7^{th}-power scaling for gain versus voltage that works well for the old glass.

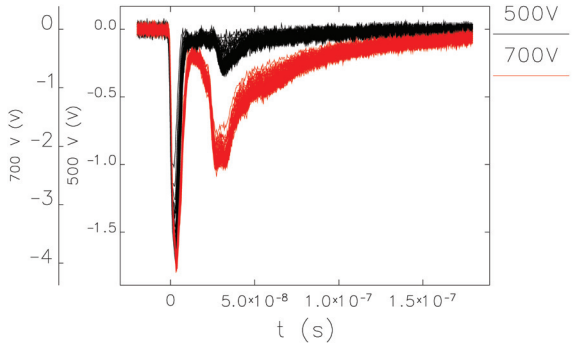

Figure 2: BLM output in the BTS with FS2 inserted showing the afterpulse for PMT biases of 500 V and 700 V.

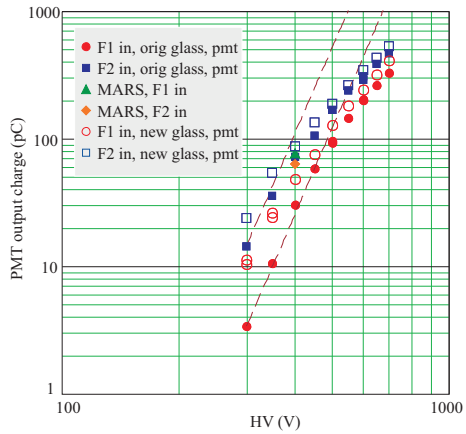

Figure 3: Measured PMT output charge vs bias voltage. Dashed lines represent the power law predictions given by $Q_o(V)=Q_{ref}\,(V/V_{ref})^n$, where $n = 7$.

Sector 35 Beamline

Gas bremsstrahlung (GB) radiation, composed almost entirely of high-energy photons, forms a narrow beam at the location of the BLM, 38 m downstream from the center of the ID straight section. The GB transverse profile is approximately round with a FWHM diameter measured to be 2 mm. A 3.2-mm thick copper plate 30 cm upstream of the BLM is used to create pair production electrons and positrons and causes the radiation to spread transversely before reaching the BLM. The radiation length of copper X_{Cu} is 12.8 g/cm^2; with a density of 8.9 g/cm^3, $t_{Cu} = X_{Cu}/\rho_{Cu}$ =1.44 cm. Thus, the copper plate represents 0.22 radiation lengths. BLM count rates are recorded during x-y scans of the radiator through the electromagnetic shower produced by the GB beam and copper plate. Figure 4(a) displays scan count rates for the radiator oriented at normal incidence to the GB beam and Fig. 4(b) at 45°. At SLAC, all LCLS BLMs are oriented normal to the electron beam axis.

MARS simulations were performed with and without an 8.2-mm-thick W shower enhancer placed just upstream of the BLM. Simulating a vertical scan of GB beam through

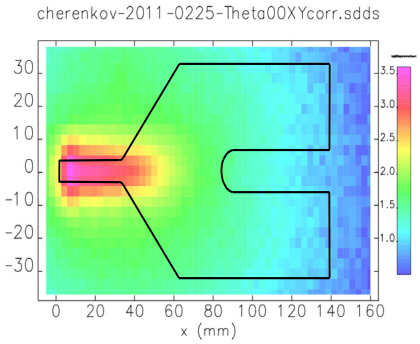

(a) 0 degrees

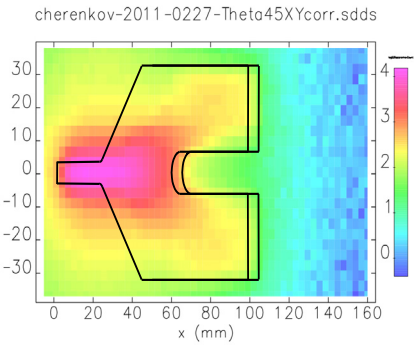

(b) 45 degrees

Figure 4: Transverse BLM scan count rate data in Sector 35 beamline hutch. Counts per second are given in a $\log_{10}$ scale. The radiator outline is superimposed over the contour plots.

the BLM radiator, fluence rate and average energy of electrons and positrons are given in Figures 5 and 6. The copper plate would produce a fluence result between the W and no-W cases, closer to that of the no-W results. The radiation length for W is 6.3 g/cm^2; with a density of 19.3 g/cm^3, the W radiation length thickness is 3.3 mm. The 8.2-mm-thick W enhancer represents 2.5 radiation lengths. The critical energy thickness in W varies from 1.0 cm at 0.2 GeV to 2.1 cm at 7 GeV.

For calibration purposes using GB radiation, the characteristics of the target gas must be known; this includes target density, $\rho_{ss}L_{ss}$, and the chemical constituency in terms of the effective atomic number, Z_{eff}. These quantities are a function of path along the beam direction, s. Average values are used in this expression. Thus, target density $\rho_{ss}L_{ss} = \int \rho(s)ds$ and average effective atomic number may be expressed as

$$\langle Z_{eff} \rangle = \frac{\int \rho(s) Z_{eff}(s) ds}{\int \rho(s) ds}. \quad (1)$$

Corrections are also be made for actual current (100 mA), current-dependent pressure, straight-section length, and $\langle Z_{eff} \rangle$. Recent measurements of GB in sector 35 with a Pb:Glass Čerenkov detector indicate $\langle Z_{eff} \rangle$=2.8; whereas, air is assumed in the simulations. The correction factor for $\langle Z_{eff} \rangle$ may be written as

$$k_Z = \frac{\langle Z_{eff1} \rangle \left(\langle Z_{eff1} \rangle + 1 \right)}{\langle Z_{eff2} \rangle \left(\langle Z_{eff2} \rangle + 1 \right)}. \quad (2)$$

In the present case, k_Z=0.175.

Measurements presented in Fig. 4(a) show a 2.5 order variation between the peak count rate and that in the large area of the radiator, suggesting a coupling efficiency of about 3×10^{-3}. The efficiency is in rough agreement with the value mentioned above; however, the GB count rates in the radiator main body are quite low. Steps to increase the count rate in this region are under investigation.

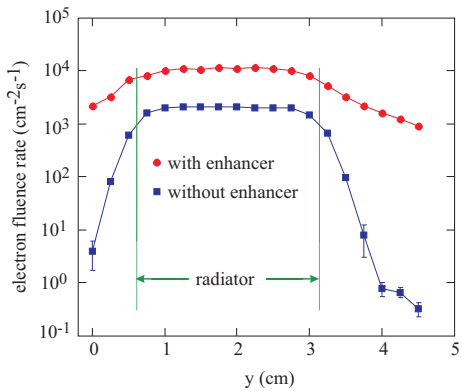

Figure 5: Simulation of e^-/e^+ fluence rates in the BLM radiator with and without tungsten.

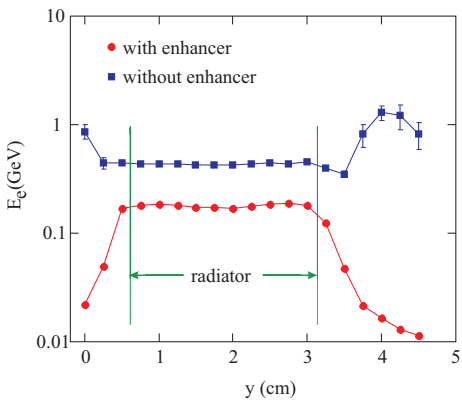

Figure 6: Simulation of average e^-/e^+ energy in the BLM radiator with and without tungsten.

REFERENCES

[1] J.C. Dooling et al. Proceedings of BIW10, Santa Fe, NM, p. 415 (2010); http://www.JACoW.org

[2] R.W. Engstrom, "Photomultiplier Handbook," RCA Corp. Report PMT-62, Lancaster, PA, p. 57, 1980.

[3] U. Akgun et al., J. Instrumentation, Technical Report 3 T01001, 2008; http://particulas.cnea.gov.ar/work-shops/icfa/wiki/images/7/76/Afterpulses02.pdf